

# FRF-Based Transient Wave Analysis for the Viscoelastic Parameters Identification and Leak Detection in Water-Filled Plastic Pipes

Bin Pan<sup>a</sup>; Huan-Feng Duan<sup>a\*</sup>;

Silvia Meniconi<sup>b</sup>; Bruno Brunone<sup>b</sup>

<sup>a</sup> *Department of Civil and Environmental Engineering, The Hong Kong Polytechnic University, Hung Hom, Kowloon, Hong Kong SAR*

<sup>b</sup> *Department of Civil and Environmental Engineering, The University of Perugia, G. Duranti 93, Perugia 06125, Italy*

\* *Corresponding author: hf.duan@polyu.edu.hk*

*Manuscript Submitted to Mechanical Systems and Signal Processing (MSSP)*

**Abstract:** Plastic/viscoelastic pipes, such as polyvinyl chloride (PVC), polyethylene (PE) and high-density polyethylene (HDPE), have been increasingly used in water piping systems, which has stimulated the study of viscoelastic hydrodynamics in these pipe systems. An in-depth understanding of the pipe-wall viscoelasticity features is beneficial and necessary to the effective application and management of plastic pipes such as leak detection in urban water supply systems. This paper presents a frequency response function (FRF)-based transient wave analysis method (TWAM) for the identification of viscoelastic pipe properties as well as the detection of leaks in water filled plastic pipes. To this end, an analytical FRF expression is firstly derived for the interaction of transients with pipe-wall elasticity and leaks in plastic pipes, which is thereafter used for the identification of viscoelastic parameters and potential leaks in plastic pipes. Laboratory experiments are performed to validate the proposed FRF-based TWAM and thereby examining the effective range of injected wave bandwidth for accurate leak detection with existence of pipe-wall viscoelasticity. The validated method is further analyzed through extensive numerical applications to systematically examine the influences of different system and flow conditions. Application results confirm the feasibility and accuracy of the developed FRF-based TWAM method for the identification of viscoelastic parameters as well as the detection of plastic pipe leaks. The results also indicate that the proposed method in this study is more accurate to locate leaks than to size leaks in plastic pipes, which requires more attention to the future applications.

*Keywords:* leak detection; transient wave analysis; plastic pipes; frequency response function (FRF); viscoelasticity; bandwidth

## 1. Introduction

Effective management of urban water infrastructures is playing an important role for the smart city development worldwide [1, 2]. However, because of the rapid deterioration and long-term operation, current urban water supply systems (UWSSs) are suffering from the leakage problem to varying degrees. In Europe, for example, it has been estimated that each year about 20% of the transported water runs away from the water infrastructure due to leakage or other factors [2]. Similarly, in Hong Kong, after an upgrading and rejuvenating program with an investment of over HK\$ 20 billion during 2000~2015, the water loss from leakages has been greatly reduced, but still keeps at around 15% of the total transported water [3]. And what's worse, the water loss starts to increase gradually after the completion of this expensive investment program.

Usually, pipe leakage in UWSS is associated with poor maintenance/operating conditions, erosion, inappropriately connecting methods and even external constructive work. When a leak exists in the system, it will not only cause the resources loss, but also increase the potential risk of invasion of pathogens and hazardous substances. Therefore, leak detection is of great practical value and significance to effectively operate and manage a UWSS. Traditionally, a pipe leak can be detected by many passive methods including commercial ones that mostly rely on different devices such as sensors, detectors, cameras or radars. However, the use of these methods is usually time consuming and inefficient, which can be evidenced by the existing critical situation of water loss in UWSSs (e.g., over 30% on average in the world) [4]. As a result, both scientists and engineers in this field have tried their best to explore new and more efficient ways for solving leakage problem in UWSSs.

Recently, many researches have demonstrated that transient flows in pipelines, which are frequently triggered and commonly existent (unavoidable) in UWSS, may be utilized for pipe condition assessment (e.g., leak detection [5] or blockage assessment [6, 7]). In this regard, this method based on transient flow analysis has been evidenced to be an efficient method for such an assessment purpose, since the transient wave can travel with very fast speed in pipes (e.g., the wave speed attains to 1000 m/s in common elastic pipes). From this perspective, this new type of method – transient wave analysis method (TWAM) – has great potential (with efficiency and accuracy improvement) for pipe condition assessment such as leak detection.

In the literature, four main different types of TWAMs have been proposed [8], namely, transient wave reflection based method (TRM) [9, 10], transient wave damping based method (TDM) [11, 12], transient frequency response function based method (FRF) [13-17] and inverse transient analysis (ITA) method [5, 18]. These methods have been widely developed and employed to identify leaks in single pipeline systems or simple networks [19]. Among these TWAMs, the frequency domain method (e.g., FRF-based method) are gaining more and more attention, as the 1D water hammer equations can be more easily solved in the frequency domain (with approximate analytics) for systems with different complexity [20-21] and more importantly, previous applications have demonstrated relatively little influence of system noises on the FRF-based method. Recently, Wang et al. further improved the frequency domain method by introducing the advanced match-field processing (MFP) technology for transient data analysis [22-26]. They found that this coupled TWAM-MFP method is robust, accurate and can maximize the signal-to-noise ratio. In addition to the single leak detection, this method has also been proven to be capable to detect multiple leaks in pipes [22-24, 26]. However, it is worthy of noting that most of leak detection methods were applied to elastic pipes only, which are commonly made of metals or concrete [10, 12, 14, 16, 17]. In fact, due to economical or other concerns, metallic/elastic pipes (e.g., standard threaded galvanized iron or steel, copper, brass, wrought iron, or cast-iron pipes) and their fittings are mainly used in small pipes in UWSSs [1]. In recent years, more and more plastic material pipes (with viscoelastic pipe-walls) have been produced and applied in urban water systems (supply and drainage), so as to provide good hydraulic and mechanic characteristics during the fluid conveying process [27].

In current UWSS, the commonly used plastic/viscoelastic pipes include: polyvinyl chloride (PVC) pipe, the polyethylene (PE) pipe, the acrylonitrile butadiene styrene (ABS) pipe, and so on. Compared with traditional elastic pipes, viscoelastic pipes, because of their special molecular structure, can continually deform even under a constant stress [28]. This kind of mechanical response is termed as the retarded response of viscoelastic materials and can be described by the creep function that consists of two sets of parameters (e.g., the creep compliance and the retardation time) [27-30]. On this point, the viscoelastic properties of plastic pipes, on one hand, can protect the pipeline from large the pressure waves/fluctuations. On the other hand, the additional damping from the retarded response may mask transient wave behavior (reflection and transmission) induced from the leaks and other associates in the

system, so that the previously developed TWAM may become inaccurate or even inapplicable for leak detection in such plastic pipes.

To address these additional effects of plastic pipe-wall on transient responses, it is necessary to accurately pre-determine and identify viscoelastic parameters before the applications of any leak detection method especially TWAM [5, 25]. To this end, viscoelastic parameters are often obtained from tests of the similar and intact pipeline system. For example, Soares et al. [5] used the non-leak pipe to identify the viscoelastic parameters and then these identified parameters were used to identify the leak location and size using the ITA method in the same system with a leak in it. Their results show that, once identified accurately, the ITA method can accurately identify the leak location (e.g., errors in predicting the leak location can be less than 3% of the total length). However, it should be noted that their viscoelastic parameters were pre-acquired from the same intact system and this method may not be valid in real systems as it may not be feasible to pre-determine these parameters from the same intact system in practice. Besides, previous studies have also shown that viscoelastic parameters are vulnerable to external conditions (e.g., stress history, constraint conditions [28, 30] and even pipe scales [31-33]), and the results from the quasi-static or intact creep tests are not accurate enough for transient wave modelling and analysis [27]. In this regard, the viscoelastic parameters are usually calibrated and determined based on the instant transient analysis of the same pipeline system under investigation so as to avoid the potential influences from other complex external factors.

In current application practice, viscoelastic parameters are commonly calibrated in the time domain [30]. Although this method can provide relatively satisfactory results for the transient modelling, the whole analysis procedure is very time consuming especially when the sampling frequency is relatively high, or the length of the data is large for practical applications [29]. Meanwhile, it has been noted from previous applications that this time domain ITA method may not be valid for viscoelastic parameter identification in a leaking system. Recently, Gong et al. [29] proposed a frequency domain method for viscoelastic parameter identification for pipeline without leakage. They found that locations of resonance peaks of transient responses are frequency dependent, and based on this, they proposed a method to identify the viscoelastic parameters. However, in their method the retardation times were artificially fixed in advance according to previous relevant researches, so that the application results may not be general to different plastic pipes, because the response time scale of different plastic pipes may be very different. To overcome this drawback, the authors

of this paper analytically identified the influence of retardation time scales as well as unsteady friction, with proposing a multistage FRF-based method for accurately identify viscoelastic parameters in a real system [34]. The results show that different retardation times could cause different frequency shifts; and thus, these shifts can be used to determine different retardation times and creep coefficients simultaneously through a stage by stage process. The proposed FRF-based transient method, on one hand, is found to be very efficient as it only uses resonance peaks and accurate as it determines simultaneously retardation time scales and creep coefficients; on the other hand, it is also more suitable to identify the viscoelastic parameters in both intact and leaking pipes. From this perspective, it is expected that this multistage FRF-based TWAM can be further extended to detect potential leaks in plastic pipes. Thus, the method extension and application are the study scope and main content of this paper.

In this paper, the multistage FRF-based TWAM is further developed and employed to identify both viscoelastic parameters and potential leaks in plastic pipes. The framework of this paper is organized as follows: following this introduction, the model and method for FRF-based TWAM development are presented, in which the application procedures of the viscoelastic parameters identification and leak detection are illustrated. Thereafter, a laboratory experimental setup is introduced, and extensive test results are applied to validate the developed FRF-based method and application procedure. The validated FRF-based method is then applied extensively to different numerical cases that cover typical ranges of system and flow conditions in the UWSS. Based on the experimental test data and numerical application results, the FRF-based TWAM is discussed for its effectiveness (accuracy and applicability) for viscoelastic parameters identification and leak detection in plastic pipes. Finally, the key results and findings from this study are concluded at the end of this paper.

## 2. Model and Method Development

### 2.1. Model Description

The continuity and momentum equations considering both retarded deformation and the friction effect of the 1D transient flow in viscoelastic pipelines are expressed as [35]:

$$\frac{gA}{a^2} \frac{\partial H}{\partial t} + \frac{\partial Q}{\partial x} + 2A \frac{\partial \varepsilon_r}{\partial t} = 0 \quad (1)$$

$$\frac{1}{gA} \frac{\partial Q}{\partial t} + \frac{\partial H}{\partial x} + \frac{\pi D}{\rho g A} (\text{sign}(Q)) \frac{\rho f Q^2}{8A^2} + \frac{4\rho v}{DA} \int_0^t W(t-t') \frac{\partial Q(t')}{\partial t'} dt' = 0 \quad (2)$$

where  $H$  and  $Q$  are piezometric head and discharge, respectively;  $g$  is gravitational acceleration;  $a$  is elastic component of wave speed of plastic pipe;  $D$  and  $A$  are internal diameter and cross-sectional area of pipe;  $\rho$  is fluid density;  $f$  is Darcy-Weisbach friction factor;  $x$  and  $t$  are the spatial and time coordinates;  $\nu$  is kinematic viscosity of the fluid;  $\varepsilon_r$  = the total circumferential retarded strain of plastic pipe-wall due to the viscoelasticity of the pipe material, which is usually described by the conceptual K-V model. In a K-V model which contains  $k$  elements, the total retarded strain can be treated as the linear superposition of each element as expressed by [30]:

$$\varepsilon_r = \sum_{k=1}^n \varepsilon_k \quad (3)$$

in which  $\varepsilon_k$  represents the retarded strain caused by the  $k^{\text{th}}$  K-V element. For a linearized K-V model, it has the form [30, 35]:

$$\varepsilon_k = \int_0^t \Psi(x, t-t') \frac{J_k}{\tau_k} e^{-\frac{t'}{\tau_k}} dt', \Psi(x, t) = C(H(x, t) - H_0(x)), C = \frac{\alpha \gamma D}{2e} \quad (4)$$

$$CJ_k H = \sum_{k=1}^n (\tau_k \frac{\partial \varepsilon_k}{\partial t} + \varepsilon_k) \quad (5)$$

where  $C$  is a lumped coefficient;  $\gamma = \rho g$  is specific weight;  $\alpha$  is pipe constraint coefficient considering both cross-sectional and axial constraint conditions;  $J_k$  = creep compliance of the  $k^{\text{th}}$  K-V element;  $\tau_k$  is retardation time of the  $k^{\text{th}}$  K-V element;  $W(\cdot)$  is the weighting function of the unsteady friction (UF) model, given by [36]:

$$W(t) = \frac{D}{4\sqrt{\nu}} \frac{e^{-\lambda t}}{\sqrt{\pi t}} \quad (6)$$

with  $\lambda$  being the UF convolution coefficient for different flow conditions, which can be calculated by the following formula:

$$\lambda = \frac{(0.54\nu R_0^{\frac{14.3}{R_0^{0.05}}})}{D^2} \quad (7)$$

in which  $R_0 = V_0 D / \nu$  is the initial Reynolds number and  $V_0$  is the initial fluid velocity in the pipe.

## 2.2. Frequency Response Function (FRF) of Transient Waves

For a small perturbation, such as flow fluctuation in UWSS, a transient system can be regarded as a linear time invariance system. In the time domain, the input signal is modified by the system impulse response function (IRF) as shown in Eq. (8) below, while in the frequency domain, each mode of the injected signal is modified by the frequency response function (FRF) as expressed in Eq. (9) below. As a result, in any dynamic system shown in Fig. 1, the measured signal becomes the combination of the input signal and the system function (e.g., IRF or FRF). The IRF and FRF are exactly consistent and both can reflect the system properties. For a defective system (e.g., a leak or a blockage in a pipeline system), the transient system response will be changed based on the IRF or FRF of the system itself. Thus, after the IRF and FRF are identified, they can be used to assess the pipe wall conditions. In this study, the FRF is employed for this purpose due to the fact that the liner convolution forms of both pipe-wall viscoelasticity in Eq. (4) and unsteady friction in Eq. (3) can be easily extracted in the frequency domain.

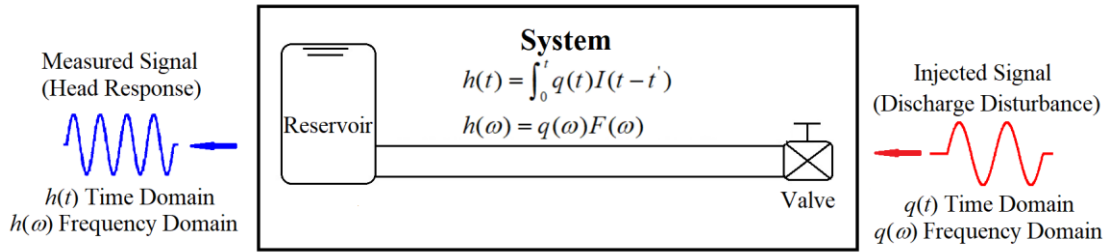


Fig. 1. the schematic diagram of the system response

$$h(t) = \int_0^t q(t')I(t-t') \quad (8)$$

$$h(\omega) = q(\omega)F(\omega) \quad (9)$$

in which  $I(\cdot)$  is the IRF in the time domain; and  $F(\cdot)$  is the FRF in the frequency domain;  $h(t)$  and  $h(\omega)$  are transient head in the time and frequency domains respectively;  $q(t)$  and  $q(\omega)$  are corresponding discharge/flowrate perturbations in the time and frequency domains respectively.

To derive the FRF for a transient pipeline system, the 1D Eqs (1) and (2) above in the time domain would be converted into their equivalence in the frequency domain. Based on the transfer matrix method [37], the FRF for an intact pipeline system can be obtained as follows:

$$\begin{pmatrix} q \\ h \end{pmatrix}^D = \begin{pmatrix} \cosh \mu_1 l & -\frac{\sinh \mu_1 l}{Z} \\ -Z \sinh \mu_1 l & \cosh \mu_1 l \end{pmatrix} \begin{pmatrix} q \\ h \end{pmatrix}^U \quad (10)$$



where  $\mu_1$  is the propagation operator which is given by Eq. (11) below;  $Z$  is the characteristic impedance and its form is shown in Eq. (12) below; the superscripts  $U$  and  $D$  denote two specific locations/boundaries in the system; and  $l$  is the length between the two locations/boundaries.

$$\mu_1 = \frac{i\omega}{a} \sqrt{\left(1 + 2\frac{a^2}{g} \sum_{k=1}^n \frac{CJ_k}{1+i\omega\tau_k}\right) \left(1 + \text{sign}(Q) \frac{fQ_0}{DAi\omega} + \frac{4\sqrt{v}}{D} \frac{1}{\sqrt{\lambda+i\omega}}\right)} \quad (11)$$

$$Z = \frac{a}{gA} \sqrt{\frac{\left(1 + \text{sign}(Q) \frac{fQ_0}{DAi\omega} + \frac{4\sqrt{v}}{D} \frac{1}{\sqrt{\lambda+i\omega}}\right)}{\left(1 + 2\frac{a^2}{g} \sum_{k=1}^n \frac{CJ_k}{1+i\omega\tau_k}\right)}} \quad (12)$$

with  $i$  being the imaginary unit ( $i^2 = -1$ ), and  $\omega$  the angular frequency.

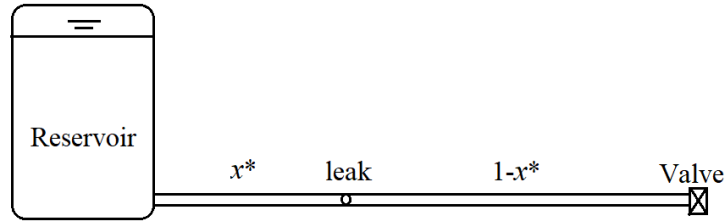


Fig. 2. the schematic diagram of the leaking system

Based on Eq. (10), the overall transform matrix of a leaking system (as shown in Fig. 2) can also be derived, which is composed of three matrixes representing two intact pipeline sections and a leaking element as shown in Fig. 2. The total length of pipe is denoted as  $L$ , and the leak location is  $x$ , so the dimensionless location of the leak is given by  $x^* = x/L$ . Thus, the field matrix of a leaking system can be expressed by Eq. (13):

$$\begin{pmatrix} q \\ h \end{pmatrix}^D = \begin{pmatrix} \cosh \mu_1 L(1-x^*) & -\frac{\sinh \mu_1 L(1-x^*)}{Z} \\ -Z \sinh \mu_1 L(1-x^*) & \cosh \mu_1 L(1-x^*) \end{pmatrix} \begin{pmatrix} 1 & -\frac{Q_l}{2H_l} \\ 0 & 1 \end{pmatrix} \begin{pmatrix} \cosh \mu_1 Lx^* & -\frac{\sinh \mu_1 Lx^*}{Z} \\ -Z \sinh \mu_1 Lx^* & \cosh \mu_1 Lx^* \end{pmatrix} \begin{pmatrix} q \\ h \end{pmatrix}^U \quad (13)$$

in which  $H_l$  = the head at the leak location in steady state;  $Q_l$  = the discharge rate of the leak in steady state;

After mathematic manipulations, the overall FRF result for a leaking pipeline system in Fig. 2 can be obtained:

$$\begin{pmatrix} q \\ h \end{pmatrix}^D = \begin{pmatrix} M_{11} & M_{12} \\ M_{21} & M_{22} \end{pmatrix} \begin{pmatrix} q \\ h \end{pmatrix}^U \quad (14)$$

in which

$$M_{11} = \cosh \mu_1 L + \frac{Q_l}{2H_l} \cosh \mu_1 L (1 - x^*) Z \sinh \mu_1 L x^* \quad (15)$$

$$M_{12} = -\frac{\sinh \mu_1 L}{Z} - \frac{Q_l}{2H_l} \cosh \mu_1 L (1 - x^*) \cosh \mu_1 L x^* \quad (16)$$

$$M_{21} = -Z \sinh \mu_1 L - \frac{Q_l}{2H_l} Z^2 \sinh \mu_1 L x^* \sinh \mu_1 L (1 - x^*) \quad (17)$$

$$M_{22} = \cosh \mu_1 L + \frac{Q_l}{2H_l} Z \cosh \mu_1 L x^* \sinh \mu_1 L (1 - x^*) \quad (18)$$

where  $M$  is the overall transform matrix element of the system; the subscript number indicates the location of the element.

For a unit transient discharge perturbation excited in the pipeline, the head response (the measured signal) at the downstream valve of a leaking system can be obtained [4, 8, 14]:

$$|h_D| = \left| \frac{\sinh \mu_1 L + \frac{Q_l}{2H_l} Z \sinh \mu_1 L x^* \sinh \mu_1 L (1 - x^*)}{\frac{\cosh \mu_1 L}{Z} + \frac{Q_l}{2H_l} \cosh \mu_1 L (1 - x^*) \sinh \mu_1 L x^*} \right| \quad (19)$$

Eq. (19) shows the head response of a leaking RPV system, which indicates that the head response is frequency dependent and is influenced by the leak information (size  $Q_l/H_l$  and location  $x^*$ ). Thus, Eq. (19) can be used to inversely identify the leak size and location by knowing or measuring the other system information and transient responses. In fact, this is the tenet of the FRF-based TWAM for leak detection. In the past, this method has been successfully applied to elastic pipes [4, 14]. However, for the leak location in the viscoelastic pipe, the characteristic impedance ( $Z$ ) and propagation operator ( $\mu_1$ ) are highly influenced by the retardation and creep parameters (e.g.,  $J$  and  $\tau$ ). Therefore, accurate identification of viscoelastic parameters becomes crucial to the effectiveness of using this FRF-based TWAM for leak detection in plastic pipelines.

### 2.3. Principle and Procedure of FRF-Based TWAM

For this study purpose, a two-step procedure of the FRF-based TWAM is proposed: (1) the viscoelastic parameters are firstly accurately determined by the formerly developed Multistage Frequency-Domain Transient-Based Method [34]; (2) based on the results of (1), the leak information can be then analyzed through the resonant peak amplitude pattern of the FRF. Specifically, many previous studies [4, 8, 14] have confirmed that a leak with reasonable size modifies only the resonance peak amplitude but has little effect on the resonant peak frequency shift. This leak-induced transient response (FRF) is very different from above viscoelastic parameters influence that presents a clear resonant frequency shift pattern. Such a difference will be the main evidence for the proposed two-step procedure for viscoelastic parameters identification and then leak detection.

**(1) Step 1: Viscoelastic parameters identification**

The resonant frequency shift pattern induced by pipe-wall viscoelasticity is used to perform the multistage method to identify the viscoelastic parameters as follows [34]:

$$(2m-1)\frac{\zeta_{EL}}{a} = \text{Im}\left(\frac{i\omega}{a} \sqrt{\left(1 + 2\frac{a^2}{g} \sum_{k=1}^n \frac{CJ_k}{1 + i\zeta_m \tau_k}\right) \left(1 + \text{sign}(Q) \frac{fQ_0}{DAi\zeta_m} + \frac{4\sqrt{v}}{D} \frac{1}{\sqrt{\lambda + i\zeta_m}}\right)}\right) \quad (20)$$

where  $\text{Im}(\cdot)$  is the imaginary part of the complex number in the bracket;  $\zeta_{EL} = \pi a/2L$  is fundamental angular frequency of an equivalent elastic pipe with the same wave speed and system configuration;  $\zeta_m$  is the  $m^{\text{th}}$  resonance peak location of experimental or numerical data from the viscoelastic pipe system. Once the resonance peak locations are extracted, the multistage procedure as described in the former study [34] is employed in this application step to efficiently identify viscoelastic parameters stage by stage.

**(2) Step 2: Leak detection**

After the accurate identification of viscoelastic parameters, the leak information in the FRF result of Eq. (19) can be inversely determined by analyzing the leak-induced transient amplitude pattern. To highlight the effect of potential leak(s) on the FRF, the difference between the transient amplitude patterns of the intact and leaking systems is utilized in this study for the leak detection, which can be expressed as follows:

$$\left(\frac{1}{|h_{leak}^D|}\right)^m - \left(\frac{1}{|h_{intact}^D|}\right)^m = \left| \frac{\frac{\cosh \mu_1 L}{Z} + \frac{Q_l}{2H_l} \cosh \mu_1 L(1-x^*) \sinh \mu_1 Lx^*}{\sinh \mu_1 L + \frac{Q_l}{2H_l} Z \sinh \mu_1 Lx^* \sinh \mu_1 L(1-x^*)} \right|^m - \left| \frac{\cosh \mu_1 x}{Z \sinh \mu_1 x} \right|^m \quad (21)$$

In Eq. (21), all other information and parameters are known from the leaking system configuration and the identification results from step 1 above, except for the leak information (size  $Q_l/H_l$  and location  $x^*$ ) which thus can be inversely detected in this step. In the meantime, the influences of different factors and parameters (such system parameters and flow conditions) are to be discussed based on the results analysis of extensive numerical applications later in this study.

#### 2.4. Performance Evaluation

The performance of the proposed method on the leak detection for both numerical and experimental tests is evaluated by the relative difference between the “real/theoretical” value and the calibrated value using Eq. (22).

$$\phi(\%) = \frac{|V_{iden} - V_{real}|}{V_{real}} \times 100\% \quad (22)$$

where  $\phi$  is the error in predicting the leak location/size;  $V_{iden}$  is the identified value of the leak location/size;  $V_{real}$  is the real/theoretical value of the leak location/size adopted in the experiment/numerical model.

### 3. Experimental Validation and Results Analysis

#### 3.1. Experimental Setup

The effectiveness of the method is firstly validated by three experimental tests which was designed and conducted in the Water Engineering Laboratory, University of Perugia, Italy (shown in Fig.3). The testing system is also an RPV system, and its configuration is the same as shown in Fig. 2. The testing system consists of a HDPE pipe (length  $L = 166.28$  m, internal diameter  $D = 0.0933$  m, thickness  $e = 0.0081$  m), a pressurized tank (at the upstream boundary, supplied by a pump to maintain a relatively constant pressure) and a downstream pneumatic valve. Transient waves for testing were generated by the fast closure of the downstream valve within a duration  $t_v$  (i.e., a step input). The leak effective area ( $(C_d A)_l$ ) in the orifice equation and other detail information are listed in Table 1, which can also be

referred to [38]. The friction factor used in simulating the intact system is calculated by the Blasius correlations (Eq. (14)) according to experiments [39]:

$$f = \frac{0.3164}{R_0^{0.25}} \quad (23)$$

in which  $R_0 = Q_0 D / A v$  is the initial Reynolds number for pipe flows.



Fig. 3. Experimental test system and facilities in the University of Perugia, Italy: (a) pressurized tank; (b) pressure transducer; (c) HDPE pipe

Table 1. Experimental test system parameters

Case no.	$A$ (m/s)	$(C_d A)_l$ (m <sup>2</sup> )	$x^*$ (-)	$Q_0$ (L/s)	$H_{tank}$ (m)	$\alpha$	$f$	$t_v$ (s)
1		6.8e-5	0.3666	4.75	19.27		0.0193	0.119
2	377.15	3.4e-5	0.3666	5.10	18.73	1.2335	0.0189	0.071
3		1.1e-4	0.7793	4.50	16.19		0.195	0.083

### 3.2. Data Processing and Results

In the validation, the head traces at the downstream valve and the tank (denoted as  $H_{tank}$ ) are recorded by pressure transducers with a sampling frequency of 1024 Hz for all the experimental test cases. For employing the FRF in the leak detection, the input signal (e.g., the valve movement or the discharge rate change) has to be quantified as the initial perturbation. For the test here, the discharge rate change is adopted as the input, which can be quantified as follows:

- the head response of the experimental data is calibrated using a sigmoid curve as shown in Eq. (24) below (Eq. (24-a). for case 1; Eq. (24-b) for case 2; Eq. (24-c) for case 3);
- the calibrated head data are used as downstream boundary conditions of the numerical intact RPV system which has the same configuration with experimental facilities;
- the input (the discharge rate change) is then obtained using the Method of Characteristics (MOC).

$$H = 17.73 + \frac{25.59}{1 + 10^{41.28(0.0701-t)}} \quad (24-a)$$

$$H = 16.12 + \frac{32.03}{1 + 10^{35.63(0.0442-t)}} \quad (24-b)$$

$$H = 15.01 + \frac{25.83}{1 + 10^{38.49(0.0463-t)}} \quad (24-c)$$

For the viscoelastic parameters identification and leak detection, the frequency response diagram (FRD) of a step input transient will induce influences to the system response from various complex factors such as nonlinear friction-wave-system interactions shown in Eq. (10) – Eq. (12) [4]. Therefore, to overcome these problems, an impulse input converted from the original data will be preferable [4, 40, 41]; thus, the corresponding initial discharges of these pulses become close to zero, so that the influence of those complex terms that are dependent on the initial discharge can be reduced as much as possible. Specifically, the influence from the friction (both steady and unsteady) is negligible for obtaining resonance peaks and FRF as the current friction models in the frequency domain are based on the initial flow state. In this study, a time-delay method is applied to convert the step signal into the corresponding impulse one (i.e., step-impulse conversion) [4]. For illustration, an initial delayed time span (DTS) of  $0.09 L/a$  is used to the measured transient data to obtain the impulse signal, so as to apply the developed method from previous research [34] for viscoelastic parameters identification. Note that the impacts of different DTSs on impulse signal conversion and detection results are to be discussed later in this paper. Identified viscoelastic parameters are shown in Table 2 and the corresponding numerical transient trace of the equivalent intact pipe system is obtained and compared with case 2 in Fig. 4. The results in Fig. 3 indicate the good accuracy, in both of transient amplitude and phase, of the proposed multistage method (Step 1) for viscoelastic parameters identification.

Table 2. The identified viscoelastic parameters of a leaking plastic pipe system

Items	$J_1$ (Pa <sup>-1</sup> )	$\tau_1$ (s)	$J_2$ (Pa <sup>-1</sup> )	$\tau_2$ (s)
Valves	$5.23 \times 10^{-11}$	0.0147	$1.49 \times 10^{-10}$	0.490

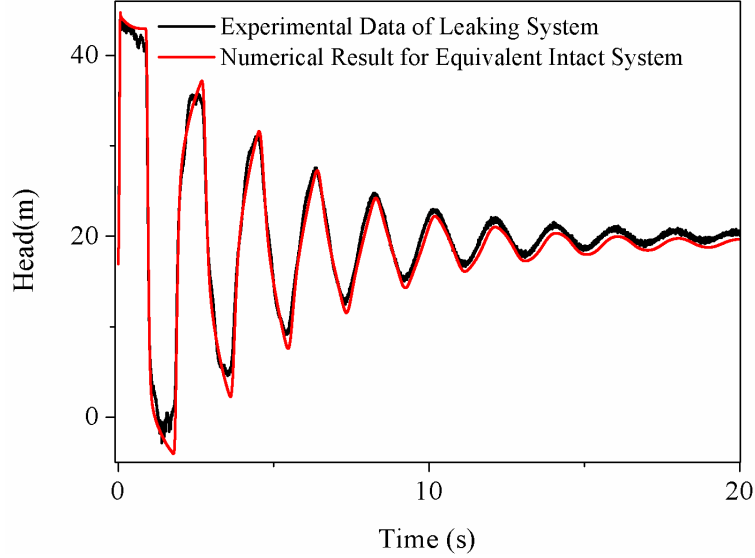


Fig. 4. Experimental measurement and numerical result for case 2

Similarly, previous studies have demonstrated an impulse signal is also preferable for TWAM [4, 40, 41, 42]. In this regard, the influence of different DTSs to the TWAM is examined and discussed in this section. The results of leak detection from extensive tests of different DTSs (from 0 ~ 4  $L/a$ ) for the above experimental test data are obtained based on the proposed TWAM (Step 2). The errors of leak information prediction (location and size) are calculated by Eq. (22) and shown in Fig. 5(a).

From the results of Fig. 5, it can be concluded that:

- (1) both the prediction errors of leak location and size are relatively large for the use of original measured data without signal conversion (i.e., DTS = 0). This is usually not acceptable for any practical application;
- (2) the use of step-impulse signal conversion may improve the leak detection results of TWAM with different degrees, which is highly dependent on the DTS;
- (3) for the applied duration of 0~4  $L/a$ , the influence of DTS can basically be divided into two regions: a relatively stable range (0.01 – 1.1  $L/a$ ), and a fluctuating range (1.1 – 4.0  $L/a$ ) that is. Clearly, the stable range of DTS that is preferable to leak detection by TWAM for this experimental test system;

(4) in the stable region ( $0 - 1.1 L/a$ ), which is enlarged in Fig. 4(b), a relatively constant improvement effect is observed for leak detection. Specifically, the error of leak location detection is within 10% and that of leak size detection is less than 20%. In fact, this result is consistent with the typical accuracy of the TWAM applications observed in the literature [18, 43].

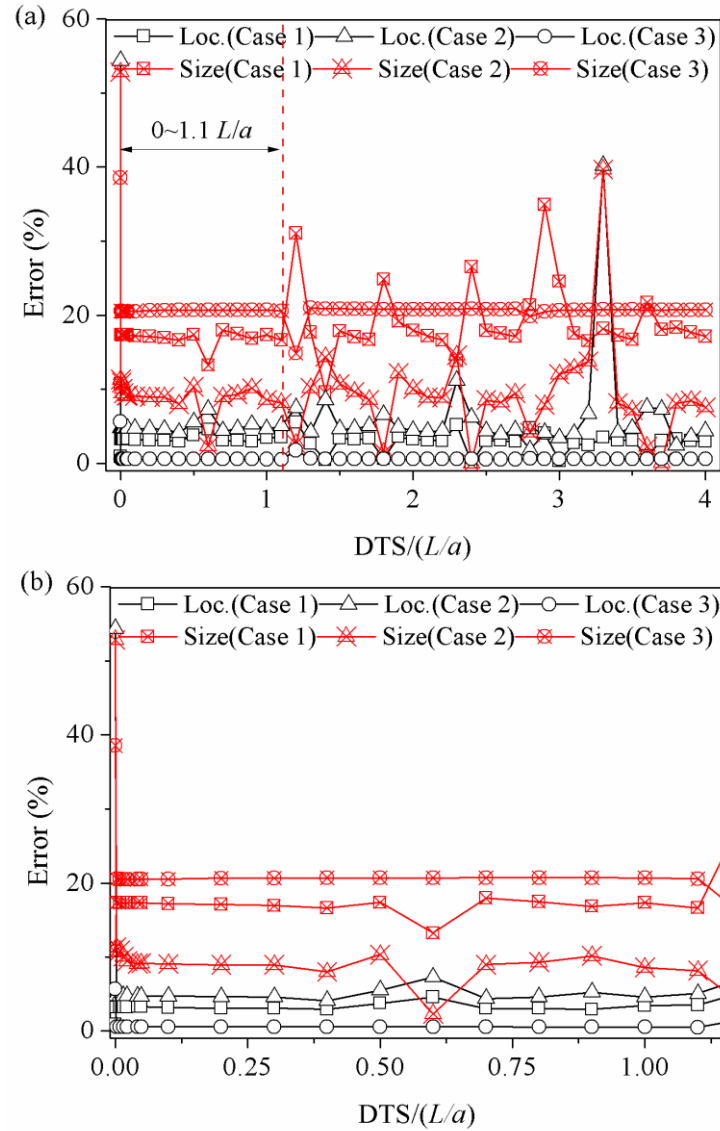


Fig. 5. Prediction errors of leak location and size (a) the overview of total tested DTSs (ranging from  $0.0 \sim 4 L/a$ ); (b) the results of DTSs which is less than  $1.1 L/a$ .

Particularly, the upper limit  $1.1 L/a$  for the effective range of the DTS for leak detection is actually equivalent to  $1.0 L/a$  in the corresponding elastic pipeline (i.e., characteristic wave time scale), considering that the wave speed of equivalent elastic pipeline (i.e.,  $a = 377.15$  m/s for elastic component calculation in Table 1) is estimated at about 1.1 times of the actual



wave speed of this viscoelastic pipeline (i.e., retarded wave speed = 349.77 m/s based on measured result of Fig. 4). That is, the effective DTS is preferable to be within the characteristic wave time scale throughout the pipeline (or the averaged wave cycle time scale along the pipeline, with an order of  $L/a$ ).

Consequently, the proposed TWAM has been verified and validated for its accuracy and effectiveness for both viscoelastic parameters identification (Step 1) and leak detection (Step 2), as long as an appropriate DTS (e.g., 0 – 1.1  $L/a$  in this test system) is applied for the transient wave analysis. It is also noted that the results and analysis above are conducted only for the specified experimental configuration and system/flow conditions. Therefore, it is necessary to systematically investigate the influences of more and different influence factors (such as initial flow and system conditions) on this method and application procedure, so as to examine and extend the applicability range as well as understand the possible limitations of the proposed method in this study.

#### 4. Extended Numerical Applications and Analysis

Based on the results of experimental validation and analysis, extensive numerical applications are performed to further examine the influences of different flow and system factors on the proposed method and procedure. Particularly, the initial flow state (i.e., initial Reynolds number,  $R_0$ ), the leaking situation (location and size), and the viscoelastic characteristics of plastic pipes are investigated in detail in this section.

##### 4.1. Numerical Test Settings

The RPV shown in Fig. 2 is adopted for numerical applications, and the basic information (fixed values) for this system is given in Table 3. Based on the results of Fig. 4 above, the transient is triggered by a discharge pulse with an equivalent DTS of 0.2  $L/a$  (i.e., pulse width) and a perturbation amplitude of 10% of the steady-state value. For inspecting the influence of flow and system conditions, only one element K-V model (with  $J_1 = 1.0e-10 \text{ Pa}^{-1}$  and  $\tau_1 = 0.1 \text{ s}$ ) are adopted in numerical tests and analysis.

Table 3. The system parameters of numerical application

Item	$a$ (m/s)	$L$ (m)	$D$ (m)	$e$ (m)	$H_{tank}$ (m)	$\alpha$	$f$
Value	385	300	0.06	0.006	40.0	1.46	0.02

To systematically investigate the impacts of different factors, the typical ranges of different factors, including leak situation (location and size) and the initial flow condition ( $R_0$ ), are given in Table 4 and applied for the extensive tests and in each evaluation. Other parameters in the system are fixed. Once generated, the transient traces are truncated to a same length. Then the creep parameters are calibrated by performing Step 1 before leak detection. It is worth noting that for the same length, the identified viscoelastic parameters ( $J$  and  $\tau$ ) are almost the same for all the numerical tests. Further analysis shows that the resonance peaks for all test cases are the same for the same data length, which reveals that the FRF is the response/function of the system and a small leak in the system cannot induce frequency shift on resonance peaks [4, 8].

Table 4. Ranges of three factors for tests

Item	Size		$x^*$	$R_0$
	$(C_dA)_l$	$(C_dA)_l/A$		
Min	$2.0 \times 10^{-7}$	$7.1 \times 10^{-5}$	0.04	$3.0 \times 10^3$
Max	$1.0 \times 10^{-5}$	0.0035	0.96	$1.27 \times 10^5$

#### 4.2. Influence of Initial Flow Condition

It is known that the transient wave generation and propagation as well as the leaking rates in water supply pipelines are highly dependent on the initial flow conditions (e.g.,  $R_0$ ). Therefore, it is necessary to evaluate the influence of such initial flow conditions on the developed leak detection method in this study. For this purpose, the leak location and size are fixed (e.g.,  $x^* = 0.327$ ,  $(C_dA)_l/A = 0.0015$  in the following study), so as to separate and highlight the individual influence of the initial flow condition from other factors in the system. Other parameters are given in Table 4. Based on the FRF-based TWAM procedure, the detection results are plotted in Fig. 6. The overall results indicate that, for most of the test cases (except the largest flow case), the initial flow condition ( $R_0$ ) affects the prediction of leak size with different degrees (e.g., error ranges from 1% to 11%), but has little influence on that of leak location (with error <1%). For the exceptional case with extremely high  $R_0$  value, by data inspection, the relatively large errors for both leak size and location predictions are mainly attributed to the very weak and distorted signal measurement of transient wave traces due to the relatively large frictional/turbulence dissipation and line packing effects along the pipeline in this system. From this perspective, it can be concluded that the developed FRF-based TWAM is

applicable to different initial flow conditions as long as the transient wave signal can be adequately sustained and well captured in the system.

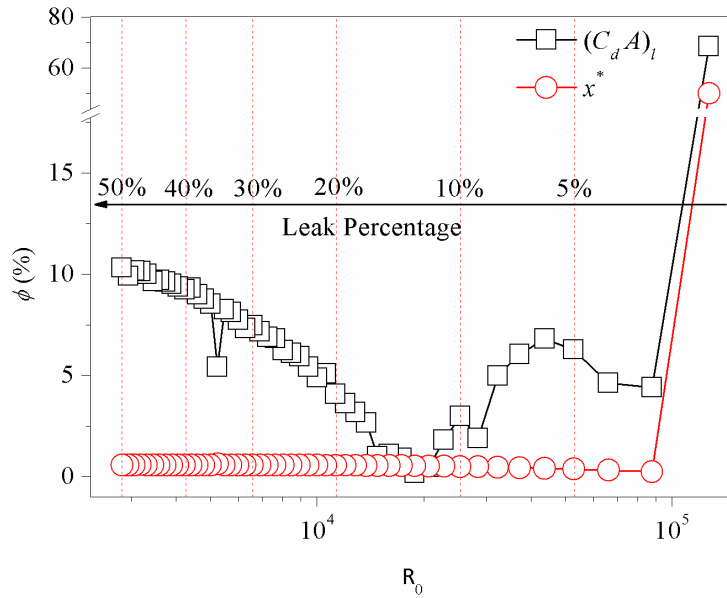


Fig. 6. Influence of initial flow conditions on FRF-based TWAM for leak detection

#### 4.3. Influence of Leaking Situation

The leak situation (e.g., leak size and location) can directly affect the propagation and modification of transient waves passing through it, and thereby inversely influencing the TWAM for its detection. In this study, the influences of leak location and size are respectively evaluated by fixing one of them when the other is under investigation. Specifically, for evaluating the influence of leak location, the dimensionless leak size  $((C_d A)_l/A)$  is fixed at 0.0015, resulting in the flowrate after the leak at 0.672 L/s, while for testing the influence of leak size, the dimensionless leak location is fixed at 0.327 and the total flowrate before the leak is 0.8 L/s. As a result, the influences of these factors on leak detection accuracy can be systematically analyzed for extensive cases by applying the FRF-based TWAM, and the results are shown in Figs. 7 (a-b).

From the results of Fig. 7, it is revealed that the performance of the TWAM for leak detection can be influenced by the actual leak information itself. Both results show that the TWAM becomes less accurate when the leak location is closer to constant-head boundaries (e.g.,  $x^* < 10\%$  for the test in Fig. 7a) and the leak size becomes smaller (e.g., leak rate  $< 5\%$  in Fig. 7b). However, the overall results of Fig. 7 demonstrate again that the prediction accuracy of leak location is much higher than that of leak size under different leaking conditions. Specifically, the average error of leak location detection is within 5%, while that

of leak size detection attains to around 15%. It is also noted that, these errors of leak detection by this TWAM are still within the acceptable ranges for practical applications. Therefore, it is confirmed that the developed multistage FRF-based TWAM is effective to the detection of different leaks (size and location) in plastic pipes, although its accuracy may be influenced within acceptable ranges (e.g., overall error < 15%) by the leak properties to be detected.

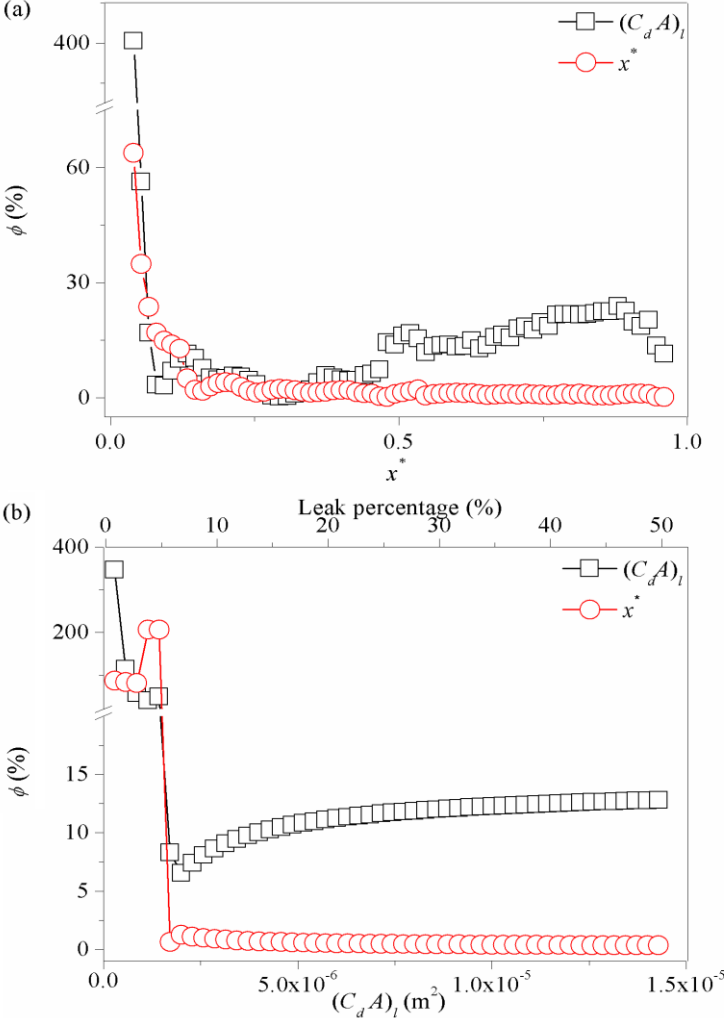


Fig. 7. Influence from different factors: (a) the change of the leak location; (b) the change of the leak size.

4.4 Influence of Viscoelastic Characteristics

In this study, the multistage FRF-based TWAM has been developed for both the viscoelastic parameters identification and leak detection in plastic pipes. Naturally, the accuracy of the first objective achievement (Step 1) will affect its subsequent application results for leak detection (Step 2). To this end, it is necessary to evaluate the influence of the viscoelastic characteristics identified in Step 1 to the leak detection in Step 2. In this regard, the possible

errors or uncertainties from the viscoelastic parameters identification will affect the following two aspects [44, 45]: (1) the simulation results of original intact system that are used as benchmark for leak detection; and (2) the calculation terms related to viscoelastic parameters that are treated as known factors in leak detection process (i.e., Eq. (19)). As a result, the accuracy of leak detection by TWAM will highly depend on the viscoelastic parameters.

To study the influence of viscoelastic parameters on leak detection, a sensitivity analysis is conducted by assuming that the viscoelastic parameters identified in Step 1 is subject to different uncertainties and random errors. For testing, a uniform distribution with a range of  $\pm 2\%$  of their “theoretical/real” values is assumed for the two viscoelastic parameters ( $\tau$  and  $J$ ). For simplicity, the mean values of the two viscoelastic parameters are fixed at  $1.0\text{e-}10 \text{ Pa}^{-1}$  ( $J_1$ ) and  $0.1 \text{ s}$  ( $\tau_1$ ), respectively. Meanwhile, the effective leak area ( $(C_d A)_l$ ) is fixed at  $4.24\text{e-}6 \text{ m}^2$ , and the initial flowrate is  $0.356 \text{ L/s}$ .

Based on the numerical settings above, extensive tests are conducted by the proposed method and the detection results are shown in Figs. 8 (a) and (b) for the prediction errors of leak location and size respectively. To clearly highlight the difference in predicting the leak location and size, the result points of which errors are less than 3% in leak location detection in Fig. 8 (a) and whose errors are less than 15% in leak size detection in Fig. 8 (b) are highlighted by red color.

Clearly, both results in Fig. 8 reveal a similar trend as the previous findings for leak detection in this study and literature. In summary:

- (1) the TWAM method is more accurate to locate leaks than to size leaks in plastic pipes, due to the relatively higher sensitivity of leak size detection to transient wave measurement accuracy;
- (2) the leak size identification becomes sensitive to the variation/uncertainties of viscoelastic parameters in the whole testing domain;
- (3) the identification results for leak location are relatively stable with a specific valley range in Fig. 8(a) where the leak location can be accurately identified (errors < 3%).

Consequently, it can be concluded from Fig. 8 that the leak detection in plastic pipes is highly dependent on the accuracy of the viscoelasticity parameters identification in advance. In this regard, the proposed multistage FRF-based TWAM in this study may provide a comprehensive option for both viscoelastic parameters identification and leak detection in plastic pipes.

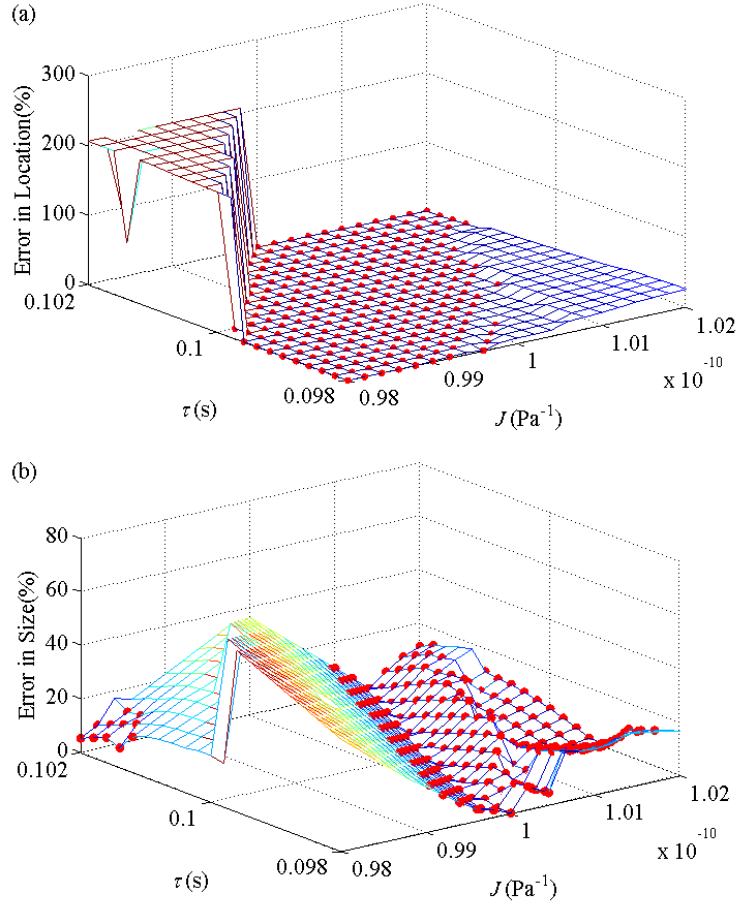


Fig. 8. Results from the identification process: (a) errors in predicting leak location; (b) errors in predicting leak size ( $J=1.0 \times 10^{-10} \text{ Pa}^{-1}$ ,  $\tau=0.1 \text{ s}$ , leaking rate = 25%).

## 5. Further Discussion on the FRF-Based TWAM

It has been evidenced in the literature that the viscoelastic parameters identification plays an important role in transient simulation of viscoelastic pipes [8, 27, 30]. The paper has experimentally and numerically validated the effectiveness of FRF-based TWAM for both viscoelastic parameters identification and leak detection. For further understanding the proposed method, the advantages, practical implementation and limitations are discussed in following parts.

### 5.1. Advantages of FRF-Based TWAM

In this study, the FRF-based TWAM is proposed to improve the efficiency of viscoelastic parameter identification. The tenet of the proposed method is to employ the invariance of resonance peak locations for viscoelastic parameter identification. This is also an advantage of this method as it does not rely on the intact system to calibrate the viscoelastic parameters. In fact, other method like Cepstrum analysis has also been a popular method for leak detection

[46, 47]. For demonstration, the proposed FRF-based TWAM is compared with the current Cepstrum analysis method, so as to further understand their different advantages and limitations for practical applications. To this end, the three experimental test cases in Table 1 are applied herein for the Cepstrum analysis, and the application results are given in Fig. 9. It is worth noting that the viscoelastic effect of pipe-wall material cannot be explicitly expressed and included in the Cepstrum, and instead, this significant damping effect is considered through the multiplication of the obtained transient amplitude by its time coordinate.

It is clearly shown from Fig. 9 that different accuracies of leak localization by the Cepstrum have been obtained for these three tests. In details, this Cepstrum analysis method has provided a very accurate result for case 1 and a relatively less accurate result for case 2 (e.g., the “real” peak was shifted a little bit), while almost failed in case 3 (e.g., the “real” peak could not be identified). Consequently, it is demonstrated herein that the Cepstrum analysis method (thus the leak detection results) may be affected with different extents by the viscoelasticity of plastic pipe-wall and other factors during transient process [46-48]. However, through these applications, it has also been observed that the Cepstrum method may have a relatively good capability on filtering the background noises from the system, which forms one of the main advantages for practical applications [46, 48].

Based on the above applications and comparisons, the main advantages of the FRF-based TWAM can be summarized as follows:

- (1) High accuracy in describing the behavior of viscoelastic pipe during transient process. Particularly, compared with the Cepstrum analysis, the inclusion of the pipe-wall viscoelasticity in the FRF-Based TWAM could enhance the accuracy of leak detection in plastic pipes. Moreover, the proposed methods can provide more information for the results of pipe diagnosis (e.g., leak size);
- (2) High efficiency in viscoelastic parameters identification and leak detection. Different from traditional calibration methods which are to minimize the difference between the original curve and the numerical results of transient wave traces, the analytical expression obtained in the FRF-Based TWAM utilizes only resonance peak locations, which may greatly enhance the analysis efficiency and accuracy as the influence of noise is relatively small at peak locations;
- (3) High accuracy in leak detection for plastic pipes. For traditional time-domain methods and other frequency domain methods (e.g., Cepstrum), the accuracy of the leak detection is highly influenced by the numerical meshing scheme or the knowledge of the system. The proposed FRF-based TWAM is a frequency domain method that

utilizing the resonance peak information rather than the whole wave signal information. As a result, this method has relatively high accuracy and tolerance to against the system noises and data measurement errors, which has been confirmed by the previous studies [8, 25, 29, 44, 49].

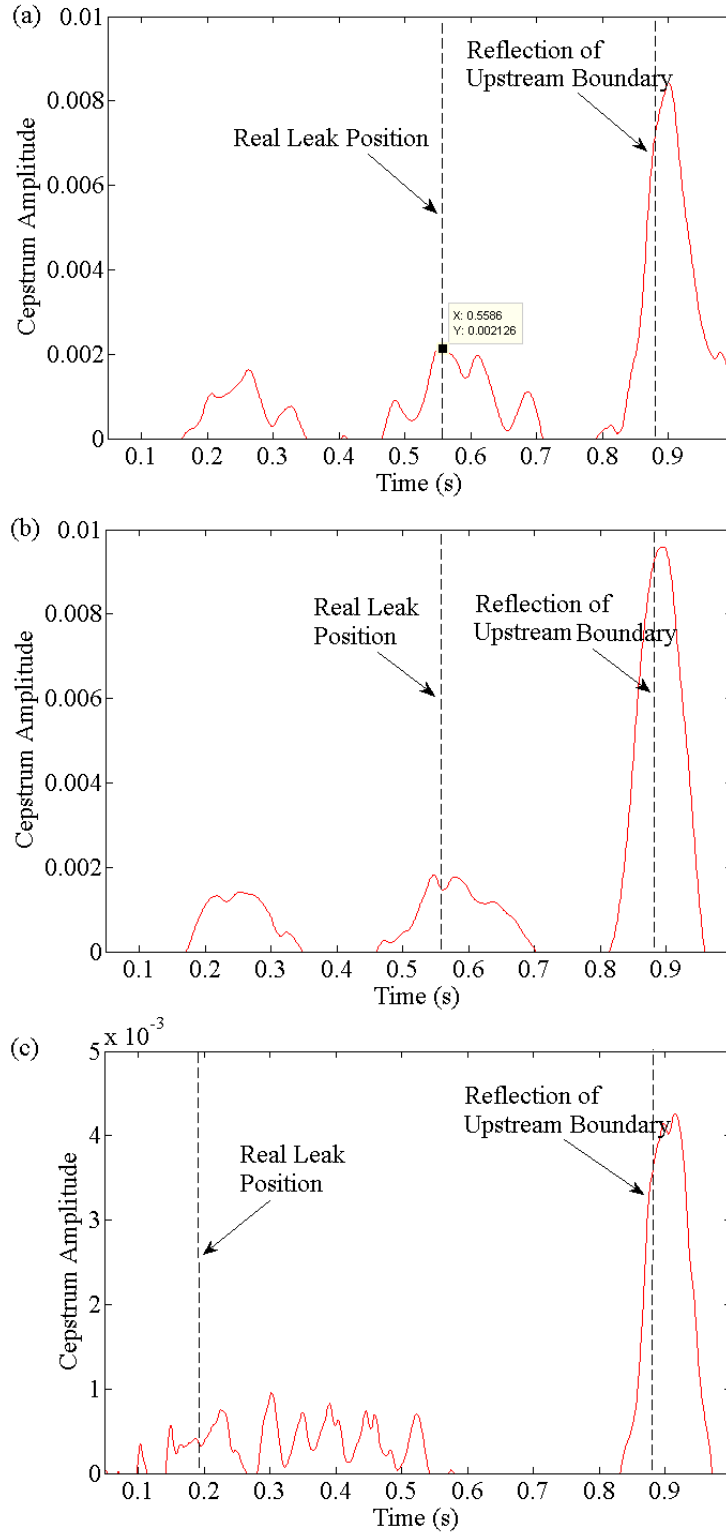


Fig. 9. Leak localization by the Cepstrum analysis: (a) case 1; (b) case 2; (c) case 3



## 5.2. Practical Implementation of FRF-based TWAM

In practical systems, the system noises may exist from white noises or un-intentionally generated sources, which may influence the whole frequency domain. Therefore, it is necessary to understand the influence ranges of system noises prior to transient signal analysis such as for viscoelastic parameters identification and leak detection. Taking one of the experimental tests (e.g., case no. 1 in Table 1) for example, the frequency spectrum results for both steady and transient states are shown in Figs. 10(a) and 10(b) respectively. It is clearly shown from Fig. 10(a) that the background noises of this test system are mainly confined to the ranges of 0-5 Hz and 30-40 Hz. In fact, these background noises in this test system are mainly from the operations of the water recycling pumps and pressurized water tanks installed in the laboratory. Meanwhile, the results of Fig. 10(b) demonstrate that the energy of the transient wave is mainly concentrated below 10 Hz in this test system. Thus, the comparison of Figs. 10(a) and 10(b) indicates that amplitude of transient peaks mainly contains the influence from relatively low frequency noises (i.e., 0-5 Hz as shown in Fig. 10(a)). It is also noted this result of noise influence ranges is only valid for the specified test system herein, while for practical applications, it is necessary to perform respective pre-analysis for the steady and transient states with different tests, so as to understand the influence ranges of the background noises in the system.

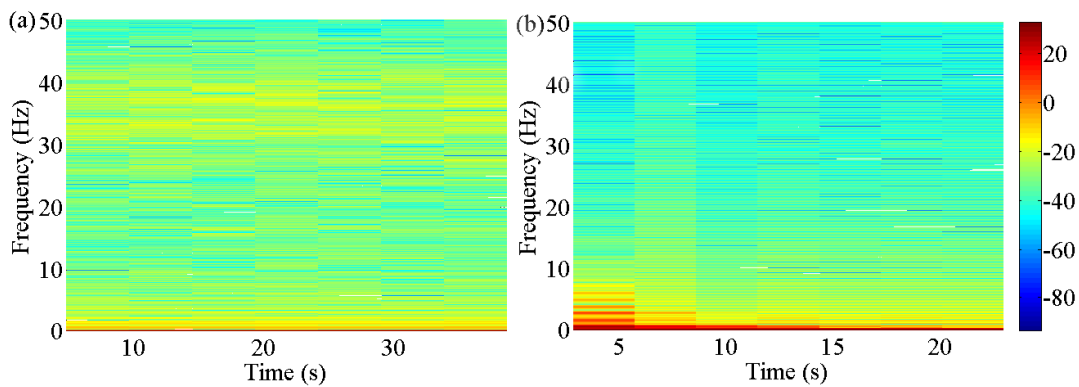


Fig. 10. Frequency spectrum graph of a leaking pipe system under: (a) steady state (background); (b) transient condition.

To overcome the influence of noise, it requires that the input signal has wide enough frequency spectrum and bandwidth, which is relevant to the DTS defined formerly in this study. For the discussed bandwidth here, it is focused on the frequency after which the magnitude of the frequency fully falls below 5% of its maximum value [4]. The results of the experimental test case no. 1 in Table 1 are shown in Figs. 11 (a)-(f), indicating clear

difference of the spectrums and bandwidths for different DTSs. For a relatively short DTS (e.g.,  $0 \sim 0.1 L/a$ ), input signals have a wide and smooth frequency spectrum as well as a broad bandwidth; afterwards, the frequency spectrum of the input signal becomes highly fluctuated and the bandwidth decreases with the increase of the DTS.

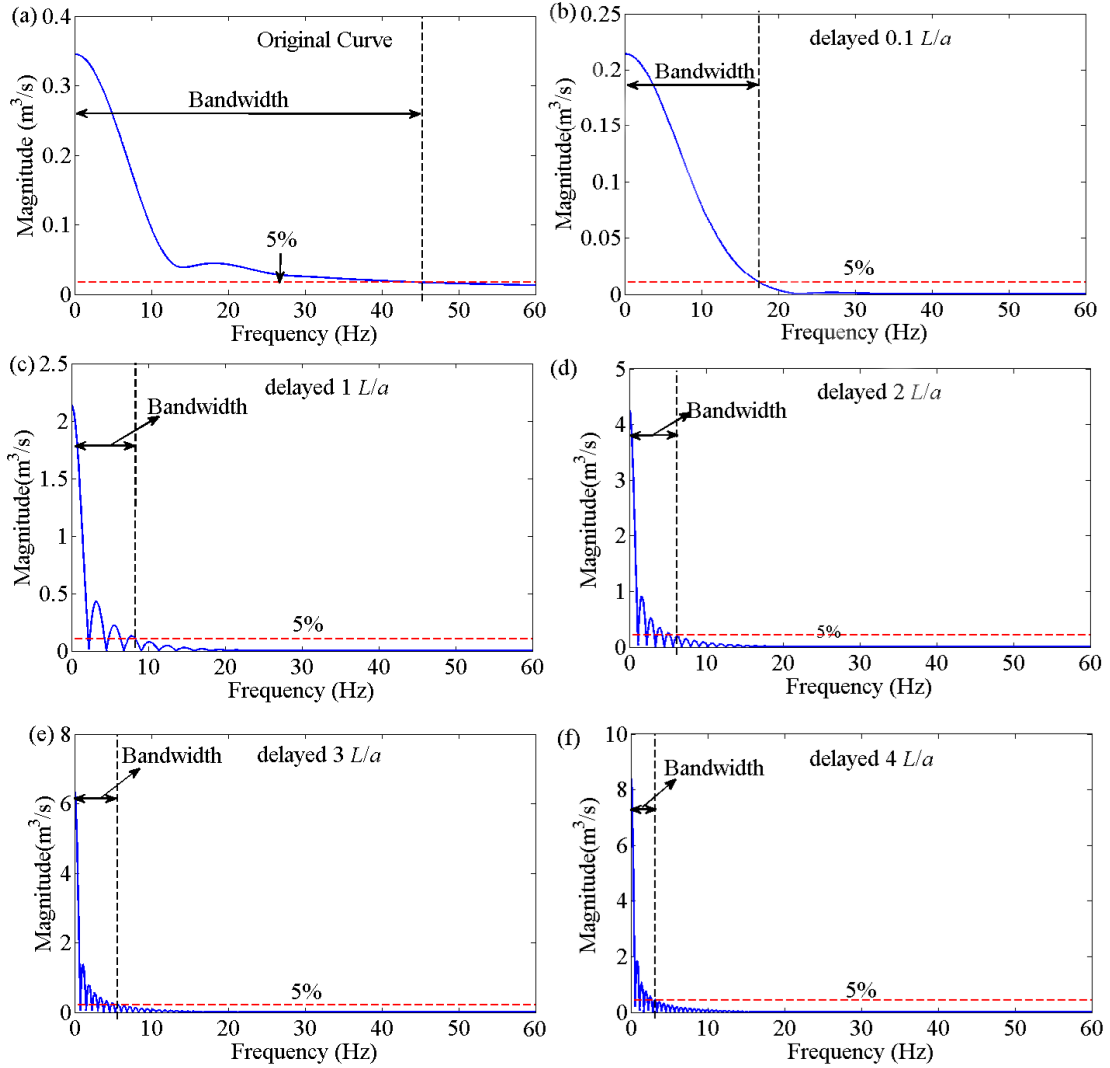


Fig. 11. Frequency spectrum and bandwidth of different input signals with different DTSs for: (a) original input (DTS = 0); (b) DTS =  $0.1 L/a$ ; (c) DTS =  $1 L/a$ ; (d) DTS =  $2 L/a$ ; (e) DTS =  $3 L/a$ ; and (f) DTS =  $4 L/a$ .

For clarity, the variation of bandwidth with the DTS is shown in Fig. 12. For an input signal which has a wide bandwidth, more frequencies of the transient system can be effectively excited and the reflection and arriving time of harmonics can be clearly identified. In fact, this is the main reason for acceptable detection results as shown in the initial stage of

Fig. 5. Thereafter, with the increase of DTS, the bandwidth of the input signal decreases, and most of the excited frequencies (especially high order harmonics) are with relatively low energy. In this circumstance, the information from leaks may be masked in noise then affect the leak detection.

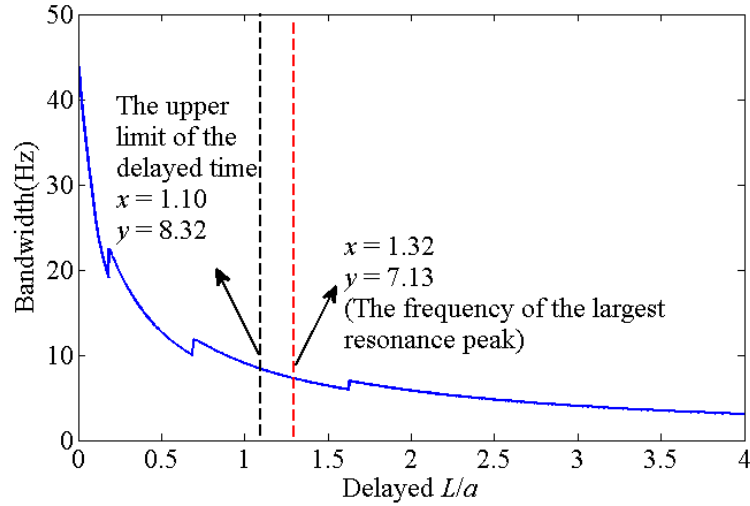


Fig. 12. Variation of input signal bandwidth with DTS

For example, for the experiment validation case no. 1 of this study, the largest measured peak is about 7.13 Hz, which corresponds to the DTS in Fig. 12 with a value of about 1.32  $L/a$ ). Based on this result, the suitable range for the DTS should be less than 1.32  $L/a$ ; otherwise, the leak detection will be affected adversely by the background noise contained in the signal. However, the calibration results in Fig. 5 show that the upper limit of the suitable delayed rang is about 1.1  $L/a$ , which corresponds to the bandwidth of about 8.3 Hz. By inspection on this studied case, this discrepancy is mainly attributed to the two following reasons. On one hand, the previous defined bandwidth may not be accurate enough under the specified threshold of 5% of the maximum value according to [4]. In this regard, a slightly higher threshold (e.g., 6~8%) may be more reasonable to define the bandwidth for this studied case herein. On the other hand, this difference indicates that an input signal with highly fluctuated spectrums may not suitable/preferable for leak detection by the FRF-based TWAM, as the energy of the resonance frequencies may be lower than the boundary of the effective bandwidth region [50]. From this perspective, it is suggested that the bandwidth of an input signal should be carefully selected in practical applications to ensure that the input have enough bandwidth to excite more effective frequencies and thus to reduce the influence from background noises.

### 5.3. Recommendations for FRF-Based TWAM Application

The tenet of the multistage FRF-based TWAM for the viscoelastic parameter identification relies on resonance peak frequency shifts caused by the viscoelastic hysteresis effects with different time scales. By taking the relatively short pipeline of the experimental test for example (e.g., length = 200 m,  $D/e = 10$ ,  $a = 400$  m/s,  $\alpha = 1$ ), the creep compliances ( $J_1 \sim J_3$ ) usually have a similar order (e.g.,  $\sim 10^{-10}$  Pa $^{-1}$ ) [25, 30]. For different retardation times, by ignoring the friction for simplicity, the frequency shifts caused by pipe-wall viscoelasticity at different resonance frequencies can be approximately calculated using Eqs. (25) and (26) below [8, 29], and the results are listed in Table 5.

$$\mu_1 = \frac{i\omega}{a} \sqrt{(1 + T_{VE})} \quad (25)$$

$$T_{VE} = \sum_{k=1}^n T_{VEk}; T_{VEk} = 2 \frac{a^2}{g} \frac{CJ_k}{1 + (\omega\tau_k)^2} \quad (26)$$

in which  $T_{VE}$  is defined as the frequency shift caused by the pipe wall viscoelasticity.

Table 5. Frequency shifts by different retardation time scales in relatively short pipe ( $L = 200$  m)

Peak Frequency	$T_{VE1}$ ( $\tau_1 = 0.05$ s)	$T_{VE2}$ ( $\tau_2 = 0.5$ s)	$T_{VE3}$ ( $\tau_3 = 1.5$ s)
0.5	0.156	0.0460	0.00688
1.5	0.131	0.00688	0.000794
2.5	0.0987	0.00255	0.000287
3.5	0.0722	0.001309	0.000146

Obviously, from Table 5, the frequency shift caused by retardation time scale is decreasing with an increase of this retardation time. As a result, at each stage of the viscoelastic parameters calibration, the influence from the pending retardation time is neglectable, so that the viscoelastic parameters can be identified one by one in the multistage FRF-based TWAM developed in this study. However, in a relatively longer pipe (e.g.,  $L = 1000$  m, other systematic parameters are the same with previous description), the frequency shifts caused by first two retardation time scales may have the same order and similar magnitude (as shown in Table 6). In this circumstance, for better using the proposed method,

it is suggested to identifying these two K-V elements simultaneously in the first stage; followed by the other K-V element calibration by fixing these first two.

Table 6. Frequency shifts by different retardation time scales in relatively long pipe ( $L = 1000$  m)

Peak Frequency	$T_{VE1}$ ( $\tau_1 = 0.05$ s)	$T_{VE2}$ ( $\tau_2 = 0.5$ s)	$T_{VE3}$ ( $\tau_3 = 1.5$ s)
0.1	0.159	0.145	0.0845
0.3	0.158	0.0844	0.0177
0.5	0.155	0.0460	0.00688
0.7	0.152	0.0273	0.00358
0.9	0.148	0.0177	0.00219

Besides, it is worth noting here that although the influence of input signal bandwidth is tested in this paper, the research is still based on a relatively simple system and only single leak is considered in the system. More complicated situations such as network or different defects and their combinations are not considered in this research. In fact, the system responses of network and different defects are expected to be very different from current study [19, 20, 50]. Nevertheless, in this study, the influence of the signal frequency spectrum and bandwidth are physically explored for explaining the different observations and results of leak detection in plastic pipes, which may be useful to future studies for complex systems.

## 6. Conclusions

This research investigates the leak detection in a viscoelastic pipe using frequency response function (FRF) based transient wave analysis method (TWAM). The analytically derived expression for the transient viscoelastic behavior and leak induced pattern in this method are adopted to identify viscoelastic parameters and detect leaks in plastic pipes. The main results and findings of this research are summarized below:

The analytical results of the FRF-based TWAM demonstrate that the pipe-wall viscoelasticity and leakage may affect the transient responses of viscoelastic pipes with different patterns. As a result, the two-step application process, coupled with a multistage calibration process, is proposed and applied for the FRF-based TWAM in this study for the viscoelastic parameters identification and leak detection respectively.

The developed FRF-based TWAM has been fully validated and verified through both laboratory experimental tests and various numerical applications. The results and analysis

confirm the effectiveness of the proposed method and application procedures. The application results also demonstrate that this method becomes more accurate for locating leaks than sizing leaks in plastic pipes, which is consistent with previous studies on elastic pipes. In the meanwhile, the accuracy of leak detection (for both leak size and location) by the proposed method in this study is acceptable for practical applications (e.g., overall < 10% for all the tests in this study)

The influences of different factors including initial flow conditions, leak information and viscoelastic parameters have been systematically investigated and discussed in the paper for the effectiveness of the proposed FRF-based TWAM. Meanwhile, the validity range of the input wave signal bandwidth has also been examined for experimental and numerical tests, which can be characterized by the defined delayed time span (DTS) in the paper. Specifically, the results show the input signal with too large DTS (e.g., greater than the characteristic wave time of the viscoelastic pipeline), thus with too small bandwidth, may not be suitable for viscoelastic parameters identification and leak detection by the TWAM. Moreover, a preferable range of DTS within the characteristic wave time scale (e.g., from 0.01 to 1.1  $L/a$  for the studied viscoelastic pipeline in this study) is suggested for the FRF-based TWAM.

Finally, the advantages and limitations of the developed FRF-based TWAM have also been discussed, with some recommendations for its practical applications provided in this paper. It is also noted that more investigations will be required to further examine the validity and applicability of the proposed FRF-based TWAM in future work.

## **Acknowledgements**

This research work was supported by the Hong Kong Research Grants Council (RGC) under projects No. 15201017 and No. 25200616, and The Hong Kong Polytechnic University under the PhD Research Studentship Scheme. In addition, supports from the Italian MIUR and the University of Perugia are acknowledged for the program “Dipartimenti di Eccellenza 2018-2022”.

## **References**

- [1] A. Roberts, *Standard Handbook of Environmental Engineering*, McGraw-Hill, New York, 1998.
- [2] C. Laspidou, ICT and stakeholder participation for improved urban water management in the cities of the future, *Water Utility Journal*, 8 (2014) 79-85.

- [3] The Water Supplies Department of the Hong Kong Government. Technical Specifications on Grey Water Reuse and Rainwater Harvesting. *Technical Report*, May 2015, pp. 50.
- [4] P.J. Lee, Using system response functions of liquid pipelines for leak and blockage detection, *PhD Dissertation*, University of Adalaide, 2005.
- [5] A.K. Soares, D.I.C. Covas, L.F.R. Reis, Leak detection by inverse transient analysis in an experimental PVC pipe system, *Journal of Hydroinformatics*, 13 (2011) 153-166.
- [6] T.C. Che, H.F. Duan, P.J. Lee, B. Pan, M.S. Ghidaoui, Transient Frequency Responses for Pressurized Water Pipelines Containing Blockages with Linearly Varying Diameters, *Journal of Hydraulic Engineering*, 144 (2018).
- [7] H.F. Duan, P.J. Lee, T.C. Che, M.S. Ghidaoui, B.W. Karney, A.A. Kolyshkin, The influence of non-uniform blockages on transient wave behavior and blockage detection in pressurized water pipelines, *Journal of Hydro-environment Research*, 17 (2017) 1-7.
- [8] H.F. Duan, P.J. Lee, M.S. Ghidaoui, Y.-K. Tung, System response function-based leak detection in viscoelastic pipelines, *Journal of Hydraulic Engineering*, 138 (2011) 143-153.
- [9] B. Brunone, Transient test-based technique for leak detection in outfall pipes, *Journal of water resources planning and management*, 125 (1999) 302-306.
- [10] S.T.N. Nguyen, J. Gong, M.F. Lambert, A.C. Zecchin, A.R. Simpson, Least squares deconvolution for leak detection with a pseudo random binary sequence excitation, *Mechanical Systems and Signal Processing*, 99 (2018) 846-858.
- [11] B. Brunone, S. Meniconi, C. Capponi, Numerical analysis of the transient pressure damping in a single polymeric pipe with a leak, *Urban Water Journal*, 15 (2018) 760-768.
- [12] X.-J. Wang, M.F. Lambert, A.R. Simpson, J.A. Liggett, J.P. Vítkovský, Leak detection in pipelines using the damping of fluid transients, *Journal of Hydraulic Engineering*, 128 (2002) 697-711.
- [13] H.F. Duan, P.J. Lee, M.S. Ghidaoui, Y.-K. Tung, Leak detection in complex series pipelines by using the system frequency response method, *Journal of Hydraulic Research*, 49 (2011) 213-221.
- [14] P.J. Lee, M.F. Lambert, A.R. Simpson, J.P. Vítkovský, J. Liggett, Experimental verification of the frequency response method for pipeline leak detection, *Journal of Hydraulic Research*, 44 (2006) 693-707.

- [15] S.H. Kim, Extensive development of leak detection algorithm by impulse response method. *Journal of Hydraulic Engineering*, 131(2005) 201-208.
- [16] C.P. Liou, Pipeline leak detection by impulse response extraction, *Journal of Fluids Engineering*, 120 (1998) 833-838.
- [17] A.M. Sattar, M.H. Chaudhry, Leak detection in pipelines by frequency response method, *Journal of Hydraulic Research*, 46 (2008) 138-151.
- [18] D. Covas, H. Ramos, Case studies of leak detection and location in water pipe systems by inverse transient analysis, *Journal of Water Resources Planning and Management*, 136 (2010) 248-257.
- [19] M. Ghazali, S. Beck, J. Shucksmith, J. Boxall, W. Staszewski, Comparative study of instantaneous frequency based methods for leak detection in pipeline networks, *Mechanical Systems and Signal Processing*, 29 (2012) 187-200.
- [20] H.-F. Duan, Transient frequency response based leak detection in water supply pipeline systems with branched and looped junctions, *Journal of Hydroinformatics*, 19 (2017) 17-30.
- [21] H.-F. Duan, Accuracy and Sensitivity Evaluation of TFR Method for Leak Detection in Multiple-Pipeline Water Supply Systems, *Water Resources Management*, 32 (2018) 2147-2164.
- [22] X. Wang, M.S. Ghidaoui, Pipeline leak detection using the matched-field processing method, *Journal of Hydraulic Engineering*, 144 (2018) 04018030.
- [23] X. Wang, M.S. Ghidaoui, Identification of multiple leaks in pipeline II: Iterative beamforming and leak number estimation, *Mechanical Systems and Signal Processing*, 119 (2019) 346-362.
- [24] X. Wang, M.S. Ghidaoui, Identification of multiple leaks in pipeline: Linearized model, maximum likelihood, and super-resolution localization, *Mechanical Systems and Signal Processing*, 107 (2018) 529-548.
- [25] X. Wang, J. Lin, A. Keramat, M.S. Ghidaoui, S. Meniconi, B. Brunone, Matched-field processing for leak localization in a viscoelastic pipe: An experimental study, *Mechanical Systems and Signal Processing*, 124 (2019) 459-478.
- [26] X. Wang, M.S. Ghidaoui, J. Lin, Identification of multiple leaks in pipeline III: Experimental results, *Mechanical Systems and Signal Processing*, 130 (2019) 395-408.
- [27] D. Covas, I. Stoianov, H. Ramos, N. Graham, C. Maksimovic, The dynamic effect of pipe-wall viscoelasticity in hydraulic transients. Part I—experimental analysis and creep characterization, *Journal of Hydraulic Research*, 42 (2004) 517-532.



- [28] A.S. Wineman, K.R. Rajagopal, *Mechanical Response of Polymers: An Introduction*, Cambridge university press, 2000.
- [29] J. Gong, A.C. Zecchin, M.F. Lambert, A.R. Simpson, Determination of the creep function of viscoelastic pipelines using system resonant frequencies with hydraulic transient analysis, *Journal of Hydraulic Engineering*, 142 (2016) 04016023.[30] D. Covas, I. Stoianov, J.F. Mano, H. Ramos, N. Graham, C. Maksimovic, The dynamic effect of pipe-wall viscoelasticity in hydraulic transients. Part II—model development, calibration and verification, *Journal of Hydraulic Research*, 43 (2005) 56-70.
- [31] M. Mitosek, M. Chorzelski, Influence of visco-elasticity on pressure wave velocity in polyethylene MDPE pipe, *Archives of Hydro-Engineering and Environmental Mechanics*, 50 (2003) 127-140.
- [32] H.F. Duan, M.S. Ghidaoui, Y.-K. Tung, Energy analysis of viscoelasticity effect in pipe fluid transients, *Journal of Applied Mechanics*, 77 (2010) 044503.
- [33] G. Pezzinga, B. Brunone, S. Meniconi, Relevance of pipe period on Kelvin-Voigt viscoelastic parameters: 1D and 2D inverse transient analysis, *Journal of Hydraulic Engineering*, 142 (2016) 04016063.
- [34] B. Pan, H. Duan, S. Meniconi, K. Urbanowicz, T. Che, B. Brunone, Multistage Frequency-Domain Transient-Based Method for the Analysis of Viscoelastic Parameters of Plastic Pipes, *Journal of Hydraulic Engineering*, 146 (2020) 04019068
- [35] H.F. Duan, M. Ghidaoui, P.J. Lee, Y.-K. Tung, Unsteady friction and visco-elasticity in pipe fluid transients, *Journal of Hydraulic Research*, 48 (2010) 354-362.
- [36] A.E. Vardy, J.M. Brown, Transient, turbulent, smooth pipe friction, *Journal of Hydraulic Research*, 33 (1995) 435-456.
- [37] M.H. Chaudhry, *Applied Hydraulic Transients*, Springer, New York, 2014.
- [38] Silvia. Meniconi, B. Brunone, Caterina. Capponi, Effect of leak size on the transient behavior of a viscoelastic pipe, *37th IAHR World Congress*, Kuala Lumpur, Malaysia 2017.
- [39] B. Brunone, A. Berni, Wall shear stress in transient turbulent pipe flow by local velocity measurement, *Journal of Hydraulic Engineering*, 136 (2010) 716-726.
- [40] M.H. Ranginkaman, A. Haghghi, P.J. Lee, Frequency domain modelling of pipe transient flow with the virtual valves method to reduce linearization errors, *Mechanical Systems and Signal Processing*, 131 (2019) 486-504.

- [41] H.-F. Duan, P.J. Lee, M.S. Ghidaoui, Y.-K. Tung, Essential system response information for transient-based leak detection methods, *Journal of Hydraulic Research*, 48 (2010) 650-657.
- [42] P.J. Lee, H.-F. Duan, J. Tuck, M. Ghidaoui, Numerical and Experimental Study on the Effect of Signal Bandwidth on Pipe Assessment Using Fluid Transients, *Journal of Hydraulic Engineering*, 141 (2015).
- [43] A. Lazhar, L. Hadj-Taïeb, E. Hadj-Taïeb, Two leaks detection in viscoelastic pipeline systems by means of transient, *Journal of Loss Prevention in the Process Industries*, 26 (2013) 1341-1351.
- [44] H.-F. Duan, Uncertainty Analysis of Transient Flow Modeling and Transient-Based Leak Detection in Elastic Water Pipeline Systems, *Water Resources Management*, 29 (2015) 5413-5427.
- [45] H. Duan, Sensitivity analysis of a transient-based frequency domain method for extended blockage detection in water pipeline systems, *Journal of Water Resources Planning and Management*, 142 (2015) 04015073.
- [46] M. Taghvaei, S. Beck, W. Staszewski, Leak detection in pipelines using cepstrum analysis, *Measurement Science and Technology*, 17 (2006) 367.
- [47] J.D. Shucksmith, J.B. Boxall, W.J. Staszewski, A. Seth, S.B. Beck, Onsite leak location in a pipe network by cepstrum analysis of pressure transients, *Journal American Water Works Association*, 104 (2012) E457-E465.
- [48] M. Ghazali, W. Staszewski, J. Shucksmith, J. Boxall, S. Beck, Instantaneous phase and frequency for the detection of leaks and features in a pipeline system, *Structural Health Monitoring*, 10 (2011) 351-360.
- [49] J. Gong, Lambert, M.F., Zecchin A.C., Simpson A.R., Experimental verification of pipeline frequency response extraction and leak detection using the inverse repeat signal, *Journal of Hydraulic Research*, 54(2016) 210-219.
- [50] S.H. Kim, Impedance method for abnormality detection of a branched pipeline system, *Water Resources Management*, 30(2016) 1101-1115.